

June 2001

Impact of the first SNO results on Neutrino Mass and Mixing

Abhijit Bandyopadhyay¹, Sandhya Choubey², Srubabati Goswami³, Kamales Kar⁴

Saha Institute of Nuclear Physics,
1/AF, Bidhannagar, Calcutta 700 064, INDIA.

ABSTRACT

We investigate the implications of the SNO charged-current (CC) and electron scattering (ES) measurements of solar 8B neutrino fluxes for neutrino mass and mixing parameters by performing a global and unified χ^2 analysis of the solar neutrino data incorporating the first SNO results along with the results from Cl, Ga and SuperKamiokande(SK) on the total flux of neutrinos as well as the recoil electron spectrum observed at SK and the CC spectrum observed at SNO in the framework of two neutrino mixing. We determine the best-fit values of the parameters, the χ^2_{min} and the goodness of fit of various oscillation solutions for both $\nu_e - \nu_{active}$ and $\nu_e - \nu_{sterile}$. We present the allowed regions in the parameter space of neutrino mass and mixing with respect to the global minimum for $\nu_e - \nu_{active}$. We compare our results with those obtained pre-SNO to highlight the impact of the SNO results.

¹abhi@theory.saha.ernet.in

²sandhya@theory.saha.ernet.in

³sruba@theory.saha.ernet.in, currently at Physical Research Laboratory, Ahmedabad-380-009

⁴kamales@tnp.saha.ernet.in

SNO has declared their first results [1] on the measurement of solar 8B neutrinos through the CC detection process



in the heavy water(D_2O) of SNO. This reaction is sensitive to only ν_e . The CC event rate as measured in SNO is

$$R_{CC} = 1.75 \pm 0.07(stat)_{-0.11}^{+0.12}(sys) \times 10^6 cm^{-2}s^{-1}$$

whereas the expectation from the standard solar model (SSM) of [2] is $5.05 \times 10^6 cm^{-2}s^{-1}$. SNO also gives the 8B flux measured by the electron scattering (ES) reaction



This reaction is sensitive to both ν_e and ν_μ or ν_τ . The ES rate measured by SNO is

$$R_{ES} = 2.39 \pm 0.34(stat)_{-0.14}^{+0.16}(sys) \times 10^6 cm^{-2}s^{-1}$$

and is in agreement with the ES rate measured by the SuperKamiokande (SK) detector [3]. These new generation high statistics experiments thus confirm the solar neutrino deficit observed in the pioneering Cl experiment [4] and subsequently in Kamiokande [5] and the low threshold Ga experiments SAGE, GALLEX and GNO [6]. A comparison of the ν_e flux measured by the CC reaction (1) with the total flux of 8B neutrinos measured at SK signifies the presence of a ν_μ and/or ν_τ component in the solar neutrino flux at 3.3σ level. The 8B neutrino flux derived from a comparison of R_{CC} and the SK observed flux is found to be $5.44 \pm 0.99 \times 10^6 cm^{-2}s^{-1}$ which is in excellent agreement with the SSM predictions [2].

In Table 1 we show the latest results for the total rates measured in Cl [4], Ga [6] and SK (1258 days) [7] and SNO (CC and ES) experiments with respect to (w.r.t) the SSM fluxes of BPB00 [2]. The numbers in the parentheses for SK and SNO are when the ν_μ or ν_τ contributions are subtracted. We also show the composition of the major fluxes in each of these experiments. For the Ga rates we give the weighted average

of SAGE, GALLEX and GNO since these measure the same quantity (neglecting the small difference in the detector latitude between SAGE and GALLEX+GNO). We do not give the older Kamiokande results which are in agreement with the SK results. The latter have much better statistics. Apart from the total rates SNO also gives the CC spectrum of the 8B neutrinos and they do not report any significant distortion with energy. SK has also published the data on the recoil electron energy spectrum in day and night and also the zenith angle spectrum [8, 9]. They also do not find any significant variation of the data with energy and although there is a slight excess of the number of events observed in the night-time when the neutrinos are passing through the earth's matter, the effect is only at 1.3σ .

Various particle physics solutions assuming non standard neutrino properties have been considered to account for the deficit [10, 11]. The simplest possibility is two flavor neutrino oscillation which requires ν_e to mix with some other flavor of neutrino. But even in this scenario there are several disconnected allowed regions in the mass-squared difference - mixing angle parameter space consistent with the global solar neutrino data. The flat recoil electron energy spectrum observed at SK has been responsible in creating a vast change in the allowed oscillation regions and their goodness of fit (GOF) as compared to those obtained pre-SK [12]. Before analyzing the SNO data it may be worthwhile to take a stock of the current situation in the simple two-flavor scenario. Two flavor oscillation analysis have been performed by various groups in the wake of the SK data [13] -[20] and certain new features became apparent. Prior to SK the best-fit to the data on total rates in Cl, Ga and Kamiokande experiments were coming in the MSW [21] SMA region. But with the flat electron energy spectrum observed in SK the best-fit in the global analysis of rates and spectrum data shifted to the LMA region. The fit in the low Δm^2 region ($10^{-7} \text{ eV}^2 - 10^{-8} \text{ eV}^2$), where earth matter effect regenerates the low energy neutrinos also became good. From the total rates data vacuum oscillation(VO) of neutrinos were allowed with $\Delta m^2 \sim 8.5 \times 10^{-11} \text{ eV}^2$ [16] . But in the global analysis with the SK electron spectrum data this became largely disfavoured as the energy dependence of the survival probability in this region

picked up conflict with the flat electron recoil energy spectrum. Recent analysis by SK [22] and other groups [18, 20] do find good fits in vacuum oscillation region for $\Delta m^2 \sim 4 - 5 \times 10^{-10} \text{ eV}^2$ where the energy averaging over the bins smears out the energy dependence of the probability and the flat spectrum observed in SK can be accounted for. However the allowed regions are very tiny around these Δm^2 values as well as somewhat fragile depending on the method of data fitting followed [18] unlike the MSW allowed regions which are quite robust against these changes. Apart from these pure MSW and pure vacuum regions a grey zone ($\Delta m^2 \sim 5 \times 10^{-10} \text{ eV}^2 - 10^{-9} \text{ eV}^2$) becomes allowed with the inclusion of the SK data, where both matter effects and the effects due to coherent oscillation phases are important. Thus there is a continuity in the allowed parameter regions and the pre-SK practice of separate analysis of the data in vacuum and MSW regions were replaced by what is called unified analysis [23] which uses a general expression for probability valid in the whole mass range $10^{-12} - 10^{-3} \text{ eV}^2$. The cutoff in the Δm^2 from above is due to the constraint from the CHOOZ reactor experiment [24]. Another new aspect is the appearance of the dark zones ($\theta > \pi/4$) [23]. In the background of this picture emerging out from detailed analysis of the available solar neutrino data several studies have been made on the expectations and implications of the SNO results [18],[25] -[28]. Now it is time to find the precise values of mass squared differences and mixing parameters by actually incorporating the SNO results in the oscillation analysis. Careful detailed analysis of the experimental results by several groups are necessary to sharpen our understandings, explore new directions and through this gradual process one hopes to find an answer to the crucial question – do neutrinos have mass and mixing?

In this paper we investigate the significance of the SNO results for neutrino mass and mixing parameters by including these in the χ^2 -analysis of the global solar neutrino data on total rates in Cl,Ga and SK experiments and the SK day/night recoil electron spectrum. The definition of χ^2 used by us is,

$$\chi^2 = \sum_{i,j} \left(F_i^{th} - F_i^{exp} \right) (\sigma_{ij}^{-2}) \left(F_j^{th} - F_j^{exp} \right) \quad (3)$$

where i, j runs over the experimental data points. Here $F_i^\alpha = \frac{T_i^\alpha}{T_i^{BPPBOO}}$ where α is *th* (for the theoretical prediction) or *exp* (for the experimental value) and T_i is the total rate in the i th experiment. We first do an analysis with the total rates given in Table 1. The F_i^{exp} is taken from Table 1. The error matrix σ_{ij} contains the experimental errors, the theoretical errors and their correlations. For evaluating the error matrix for the total rates case we use the procedure described in [29]. The details of the code used by us can be found in [16, 17, 11]. For the rate of (ν_e -d) CC events recorded in the SNO detector we use

$$R_{CC} = \frac{\int dE_\nu \lambda_{\nu_e}(E_\nu) \sigma_{CC}(E_\nu) \langle P_{ee} \rangle}{\int dE_\nu \lambda_{\nu_e}(E_\nu) \sigma_{CC}(E_\nu)} \quad (4)$$

$$\sigma_{CC} = \int_{E_{A_{th}}} dE_A \int_0^\infty dE_T R(E_A, E_T) \frac{d\sigma_{\nu_{ed}}(E_T, E_\nu)}{dE_T} \quad (5)$$

where λ_{ν_e} is the normalized 8B neutrino spectrum, $\langle P_{ee} \rangle$ is the time averaged ν_e survival probability, $d\sigma_{\nu_{ed}}/dE_T$ is the differential cross section of the ($\nu_e - d$) interaction [30], E_T is the true and E_A the apparent(measured) kinetic energy of the recoil electrons, $E_{A_{th}}$ is the detector threshold energy which we take as 6.75 MeV and $R(E_A, E_T)$ is the energy resolution function for which we use the expression in [1]. The expression for ν_e survival probability according to an unified formalism over the mass range $10^{-12} - 10^{-3}$ eV² and for the mixing angle θ in the range $[0, \pi/2]$ is well documented [23, 31] and can be expressed as

$$\begin{aligned} P_{ee} = & P_\odot P_\oplus + (1 - P_\odot)(1 - P_\oplus) \\ & + 2\sqrt{P_\odot(1 - P_\odot)P_\oplus(1 - P_\oplus)} \cos \xi \end{aligned} \quad (6)$$

where P_\odot denotes the probability of conversion of ν_e to one of the mass eigenstates in the sun and P_\oplus gives the conversion probability of the mass eigenstate back to the ν_e state in the earth. All the phases involved in the Sun, vacuum and inside Earth are included in ξ . This most general expression reduces to the well known MSW (the phase ξ is large and averages out) and vacuum oscillation limit (matter effects are absent and the phase ξ is important) for appropriate values of $\Delta m^2/E$. The procedure which we

use for calculating P_{\oplus} and P_{\odot} in MSW, vacuum as well as the in between quasivacuum regions where both ξ and matter effects are relevant is discussed in [20].

The results for the analysis of total rates for $\nu_e - \nu_{active}$ are presented in Table 2. As far as the pre-SNO total rates are concerned both SMA and vacuum oscillation give good fits with the best-fit coming in the SMA region. For post-SNO the best-fit comes in the VO region. However the noticeable thing is that with the inclusion of the SNO data the GOF of both SMA and VO becomes worse and that in the LMA region becomes better. The non-monotonic dependence of the probability on energy in the VO and the SMA region could explain the mismatch between Cl, SK and Ga rates and good fits were obtained in these regions. Studies have shown that an enhanced mismatch between Cl and SK prefers the SMA solution [19]. Since with SNO we get one point which has a lesser mismatch with Cl than SK, the GOF of the SMA solution goes down. In the LMA region the survival probabilities of the high energy neutrinos are given as

$$P_{ee}^{LMA} \approx \frac{1}{2}(1 - \epsilon) + f_{reg} \quad (7)$$

where $\epsilon = \cos 2\theta$ and $f_{reg} = P_{2e} - \sin^2 \theta$, P_{2e} being the probability of conversion of the propagating mass eigenstate 2 to the flavour state ν_e at the detector. Since 3 of the experiments which are mainly sensitive to 8B neutrinos are now close, they can be well described through a single eq. (7) and the GOF of the LMA solution becomes better. For low energies relevant for Ga the matter effects are weak and

$$P_{ee}^{LMA} \approx \frac{1}{2}(1 + \epsilon^2) \quad (8)$$

which gives a greater probability as compared to eq.(7) for the same ϵ and the rates of Table 1 are accounted for.

These features are reflected in figs. 1 and 2 where we plot the allowed regions for pre-SNO and post-SNO (excluding ES scattering) respectively at 90% ($\chi^2 \leq \chi_{min}^2 + 4.61$) 95% ($\chi^2 \leq \chi_{min}^2 + 5.99$) and 99% C.L. ($\chi^2 \leq \chi_{min}^2 + 9.21$) from an analysis of total rates. Since the GOF improves for LMA, the allowed region becomes slightly bigger.

In Table 3 we present the best-fit values of parameters, χ_{min}^2 and the GOF of the

solutions for the $\nu_e - \nu_{sterile}$ solution from an analysis of total rates. Since R_{CC}^{SNO} is significantly lower than R_{ES}^{SK} pure $\nu_e - \nu_{sterile}$ transitions are highly disfavoured and this is responsible for the bad fit obtained in Table 3 after including the SNO results.

For the global analysis the total χ^2 is defined as

$$\chi_{tot}^2 = \chi_{rates}^2 + \chi_{skspec}^2 + \chi_{snospec}^2 \quad (9)$$

where χ_{skspec}^2 and $\chi_{snospec}^2$ are the χ^2 for the SK recoil electron spectrum and SNO CC spectrum respectively and χ_{rates}^2 corresponds to the χ^2 from the total rates data. For the calculation of the rates part i,j runs from 1 to 4 if we do not include the ES rate measured in SNO and 1 to 5 if we include the ES rate from SNO; for the SK spectrum part i,j runs from 1 to 38 corresponding to 19 day and 19 night bins; for the SNO CC spectrum i,j runs from 1 to 11. To account for the fact the ES rate measured in SK is not independent of the spectrum we vary the normalisation of the spectrum as a free parameter. Similarly for SNO CC spectrum we introduce a free normalisation for the spectrum to avoid overcounting with the total CC rate. For the calculation of the error matrix for the SK spectrum we include the statistical error, correlated and uncorrelated systematic errors and the error due to the calculation of the spectrum [8, 22]. For the SNO CC spectrum we include the statistical error and the correlated systematic errors from [1]. For all our analyses presented in this paper we keep the 8B flux fixed at SSM value.

The no-oscillation $\chi^2/d.o.f$ is 100.31/52 which is disfavored at 99.99% C.L. from the global data. In Table 4 we show the results of global analysis of the rates and the spectrum data for oscillation to an active flavour. For understanding the impact of the SNO data we present the results for cases with and without SNO. For the case with SNO we perform the analysis including and excluding the SNO CC spectrum and ES data. The pre-SNO analysis indicate that with the inclusion of the SK day/night spectrum data the GOF of the SMA solution becomes worse and fit in the LMA and LOW regions become much better, with LMA giving the best-fit. This worsening of fit in the SMA region is owing to the fact that the peculiar energy dependence of the observed rates in Cl, Ga and SK experiments favour larger values of $\tan^2 \theta$ (the non-adiabatic regime)

while the flat recoil electron energy spectrum observed by SK prefers smaller values of $\tan^2 \theta$. For VO case also the rates data require a $\Delta m^2 \sim 8 - 9 \times 10^{-11} eV^2$ while the flat SK spectrum requires a $\Delta m^2 \sim 4.5 \times 10^{-10} eV^2$ for which energy averaging gives an approximately constant probability for the high energy neutrinos. In this tug-of-war between the rates and SK spectrum data the fit in VO region become worse for the global analysis and the allowed regions from rate only analysis largely disappear [20, 18, 14]. LMA and LOW on the other hand can describe the flat recoil electron spectrum at SK very well and the GOF in these regions are much better.

The inclusion of the total SNO CC rate enhances the conflict between the rates and SK spectrum data in the SMA region. If we look at the post-SNO χ^2_{min} in Table 4 for the case excluding the SNO CC spectrum and the ES data then we find that it is the SMA region which becomes more disfavoured with SNO, while all the others are seen to improve. The effect of addition of the SNO CC spectrum in the analysis is to increase the $\chi/d.o.f$ and hence reduce the GOF for all the solutions in general. However due to large errors, both statistical as well as systematic, the SNO spectrum fails to make any significant change in the relative fit between the different solutions.

In fig. 3 we show the allowed regions at 90%, 95% and 99% C.L. obtained from the global analysis for $\nu_e - \nu_{active}$ transitions including all published SNO data. The only significant change in the allowed regions after including the SNO results is the disappearance of the SMA region at 99% C.L. as a result of the increased conflict between the total rates and SK spectrum data ⁵.

In Table 5 we present the results of global analysis for $\nu_e - \nu_{sterile}$ solution and as expected the fits become worse with the inclusion of SNO results.

To summarise, the recent SNO results are very important for both particle physics and astrophysics. Comparison of the ES(CC+NC) rate measured at SK with the CC rate measured by eq. (1) in SNO give statistically significant data on the NC component of the solar ν_e flux and the no-oscillation hypothesis is disfavoured at 99.99% C.L.. The solar 8B ν_e flux from the SNO CC measurements together with the ν_μ or ν_τ flux inferred

⁵ The pre-SNO contours for global analysis using our code are given in [20].

in conjunction with the ES rate measured at SK give excellent agreement with the predicted 8B flux from the SSM of [2].

We include the recent SNO results in global χ^2 analysis of the solar neutrino data. We find that inclusion of the SNO CC data in the analysis of *total rates* worsens the GOF of the SMA solution and betters the GOF of the LMA solution. The increased mismatch between the total rates data and SK spectrum data due to the inclusion of the SNO CC rate further disfavours the SMA solution and we get no allowed region even at 99% C.L. from the global fit. The sterile neutrino alternative gets highly disfavoured by the rates analysis and the global analysis gives a GOF of only 15% in the SMA region. However for an arbitrary 8B flux normalisation, a small admixture with the sterile neutrino state cannot be ruled out completely as is shown by the model-independent analysis performed in [32].

Note added: When we were completing our analysis the paper [33] came on net. This covers some part of the analysis performed in this paper and the results are in broad agreement.

The authors would like to thank D.P. Roy for his valuable comments and suggestions. S.G. would like to thank the theory group of Physical Research Laboratory for their hospitality.

References

- [1] Q.R. Ahmad *et al.*, <http://www.sno.phy.queensu.ca/sno/firstresults/>, nucl-ex/0106015.
- [2] J.N. Bahcall, S. Basu, M. Pinsonneault, astro-ph/0010346.
- [3] Y. Fukuda *et al.* (The Super-Kamiokande collaboration), Phys. Rev. Lett. **81**, 1158 (1998); erratum **81**, 4279 (1998).
- [4] B.T. Cleveland *et al.* Astrophys. J **496**, 505 (1998).

- [5] Y. Fukuda *et al.*, (The Kamiokande collaboration), Phys. Rev. Lett. **77**, 1683 (1996).
- [6] J.N. Abdurashitov *et al.*, (The SAGE collaboration), Phys. Rev. Lett. **77**, 4708 (1996); Phys. Rev. **C 60**, 055801 (1999); W. Hampel *et al.*, (The Gallex collaboration), Phys. Lett. **B388**, 384 (1996); Phys. Lett. **bf B447**, 127 (1999); Talk presented in Neutrino 2000 held at Sudbury, Canada (T.A. Kirsten for The Gallex collaboration), Nucl. Phys. **B** Proc. Suppl. **77**, 26 (2000); M. Altmann *et al.*, (The GNO collaboration), Phys. Lett. **bf B492**, 16 (2000); Talk presented in Neutrino 2000 held at Sudbury, Canada (E. Bellotti for the GNO Collaboration) Nucl. Phys. **B** Proc. Suppl. **91** 44 (2001).
- [7] Y. Fukuda *et al.*, Phys. Rev. Lett. **86**, 5651 (2001).
- [8] Y. Fukuda *et al.* (The Super-Kamiokande collaboration), Phys. Rev. Lett. **82**, 2430 (1999).
- [9] Y. Fukuda *et al.* (The Super-Kamiokande collaboration), Phys. Rev. Lett. **82**, 1810 (1999).
- [10] S. Choubey, S. Goswami, D. Majumdar, Phys. Lett. **B484**, 73 (2000). O.G. Miranda, C. Peña-Garay, T.I. Rashba, V.B. Semikoz, J.W.F. Valle, Nucl. Phys. **B595**, 360 (2001); D. Majumdar, A. Raychaudhuri and A. Sil, Phys. Rev. **D63**, 073014 (2001); A.M. Gago, H. Nunokawa and R. Zukanovich Funchal, Nucl. Phys. Proc. Suppl. **100**, 68 (2001); M.M. Guzzo, H. Nunokawa, P.C. de Holanda, O.L.G. Peres, hep-ph/0012089; J. Pulido, hep-ph/0106201.
- [11] A. Bandyopadhyay, S. Choubey, S. Goswami, Phys. Rev. **D63**, 113019 (2001).
- [12] J.N. Bahcall, P.I. Krastev, Phys. Rev. **D53**, 4211 (1996) and references therein
- [13] J.N. Bahcall, P.I. Krastev and A.Yu. Smirnov, Phys. Rev. **D58**, 096016 (1998).

- [14] M.C.Gonzalez-Garcia and C. Peña-Garay, Nucl. Phys. Proc. Suppl. **91**, 80 (2000);
M.C. Gonzalez-Garcia, P.C. de Holanda, C. Peña-Garay, and J.W.F. Valle, Nucl. Phys. **B573**, 3 (2000).
- [15] V. Barger and K. Whisnant, Phys. Lett. **B456**, 54 (1999).
- [16] S. Goswami, D. Majumdar and A. Raychaudhuri, hep-ph/9909453.
- [17] S. Goswami, D. Majumdar and A. Raychaudhuri, Phys. Rev. **D63**, 013003 (2001).
- [18] J.N. Bahcall, P.I. Krastev, and A.Yu. Smirnov, JHEP **0105**, 015 (2001).
- [19] S. Choubey, S. Goswami, N. Gupta and D.P. Roy, hep-ph/0103318, to appear in Phys. Rev. **D**.
- [20] S. Choubey, S. Goswami, K. Kar, A.R. Antia, S.M. Chitre, hep-ph/0106168.
- [21] L. Wolfenstein, Phys. Rev. **D34**, 969 (1986); S.P. Mikheyev and A.Yu. Smirnov, Sov. J. Nucl. Phys. **42(6)**, 913 (1985); Nuovo Cimento **9c**, 17 (1986) .
- [22] Y.Fukuda *et al.* Phys. Rev. Lett. **86**, 5656 (2001).
- [23] A.de. Gouvea, A. Friedland, H. Murayama, Phys.Lett.**B490**, 125, (2000).
- [24] M. Apollonio et al., Phys. Lett. B446, 415 (1999).
- [25] J. N. Bahcall, P.I. Krastev , A. Yu. Smirnov JHEP **0105**, 015 (2001).
- [26] J.N. Bahcall , P. I. Krastev, A. Yu. Smirnov Phys. Rev. **D63**, 053012 (2001).
- [27] J. N. Bahcall, P.I. Krastev , A. Yu. Smirnov, Phys.Rev. **D62**, 093004, (2000).
- [28] V. Barger, D. Marfatia, K. Whisnant and B.P. Wood, hep-ph/0104095.
- [29] G.L. Fogli and E. Lisi, Astropart. Phys. **3**, 185 (1995).
- [30] S. Nakamura, T. Sato, V. Gudkov and K. Kubodera, Phys. Rev. **C63**, 034617 (2001).

- [31] G.L. Fogli, E. Lisi, D. Montanino, A. Palazzo , Phys. Rev. **D62**, 113004, (2000).
- [32] V. Barger, D. Marfatia and K. Whisnant, hep-ph/0106207.
- [33] G.L. Fogli, E. Lisi, D. Montanino and A. Palazzo, hep-ph/0106247.

Table 1: The ratio of the observed solar neutrino rates to the corresponding BPB00 SSM predictions used in this analysis.

experiment	$\frac{obsvd}{BPB00}$	composition
Cl	0.335 ± 0.029	B (75%), Be (15%)
Ga	0.584 ± 0.039	pp (55%), Be (25%), B (10%)
SK	0.459 ± 0.017 ($0.351 \pm .015$)	B (100%)
SNO(CC)	0.347 ± 0.027	B (100%)
SNO(ES)	0.473 ± 0.074 (0.368 ± 0.074)	B (100%)

Table 2: The best-fit values of the parameters, χ^2_{min} , and the goodness of fit from an analysis of the total rates given in Table 1 for $\nu_e - \nu_{active}$.

	Nature of Solution	Δm^2 in eV ²	$\tan^2 \theta$	χ^2_{min}	Goodness of fit
pre-SNO	SMA	5.96×10^{-6}	1.39×10^{-3}	0.30	58.39%
	LMA	2.4×10^{-5}	0.31	2.91	8.8%
	LOW-QVO	1.34×10^{-7}	0.64	7.49	0.62%
	VO	8.79×10^{-11}	0.43	0.32	57.16%
post-SNO	SMA	6.12×10^{-6}	1.46×10^{-3}	2.98	39.47%
	LMA	2.29×10^{-5}	0.32	3.32	34.07%
	LOW-QVO	1.39×10^{-7}	0.41	8.0	4.6%
	VO	7.94×10^{-11}	0.27	2.61	45.57%
without SNO ES	SMA	6.13×10^{-6}	1.46×10^{-3}	2.97	22.65%
	LMA	2.3×10^{-5}	0.32	3.26	19.59%
	LOW-QVO	1.4×10^{-7}	0.7	7.88	1.93%
	VO	7.95×10^{-11}	0.27	2.20	33.29%

Table 3: The best-fit values of the parameters, χ^2_{min} , and the goodness of fit from an analysis of the total rates given in Table 3 for $\nu_e - \nu_{sterile}$.

Nature of Solution		Δm^2 in eV ²	$\tan^2 \theta$	χ^2_{min}	Goodness of fit
pre-SNO	SMA	4.43×10^{-6}	1.44×10^{-3}	1.97	16.04%
	LMA	6.41×10^{-5}	0.58	17.45	2.94×10^{-3} %
	LOW-QVO	1.49×10^{-7}	0.85	18.01	2.19×10^{-3} %
	VO	8.99×10^{-11}	0.36	2.70	10.03%
post-SNO	SMA	4.37×10^{-6}	9.89×10^{-4}	7.91	4.79%
	LMA	6.63×10^{-5}	0.54	20.50	1.3×10^{-2} %
	LOW-QVO	2.92×10^{-8}	0.84	17.73	4.99×10^{-2} %
	VO	7.95×10^{-11}	0.30	6.62	8.5%

Table 4: The best-fit values of the parameters, χ^2_{min} , and the goodness of fit from the global analysis of rate and spectrum data with and without the SNO results for $\nu_e - \nu_{active}$.

	Nature of Solution	Δm^2 in eV ²	$\tan^2 \theta$	χ^2_{min}	Goodness of fit
pre-SNO	SMA	5.48×10^{-6}	4.88×10^{-4}	43.59	24.57%
	LMA	5.08×10^{-5}	0.35	34.73	62.14%
	LOW-QVO	1.55×10^{-7}	0.66	38.50	44.66%
	VO	4.55×10^{-10}	0.44	37.80	47.86%
post-SNO (all data)	SMA	5.4×10^{-6}	4.3×10^{-4}	59.14	17.63%
	LMA	4.45×10^{-5}	0.36	49.42	49.66%
	LOW-QVO	1.53×10^{-7}	0.68	52.59	37.40%
	VO	4.53×10^{-10}	2.94	55.70	26.9%
post-SNO (excluding SNO CC spectrum and ES)	SMA	5.36×10^{-6}	4.15×10^{-4}	45.21	22.85%
	LMA	4.45×10^{-5}	0.36	34.98	65.38%
	LOW-QVO	1.56×10^{-7}	0.69	38.38	49.8%
	VO	4.54×10^{-10}	2.35	37.83	52.31%

Table 5: The best-fit values of the parameters, χ^2_{min} , and the goodness of fit from the global analysis of rates and spectrum data for the sterile neutrino case.

		Nature of Solution	Δm^2 in eV ²	$\tan^2 \theta$	χ^2_{min}	Goodness of fit
pre-SNO	SMA	4.03×10^{-6}	4.9×10^{-4}	44.11	22.9%	
	LMA	6.09×10^{-5}	0.56	47.15	14.67%	
	LOW-QVO	3.08×10^{-8}	0.85	47.16	14.65%	
	VO	4.54×10^{-10}	0.39	41.37	32.57%	
post-SNO (all data)	SMA	4.0×10^{-6}	4.47×10^{-4}	60.41	14.87%	
	LMA	7.64×10^{-5}	0.51	63.94	8.89%	
	LOW-QVO	3.05×10^{-8}	0.87	64.38	8.30%	
	VO	4.67×10^{-10}	0.28	65.01	7.52%	

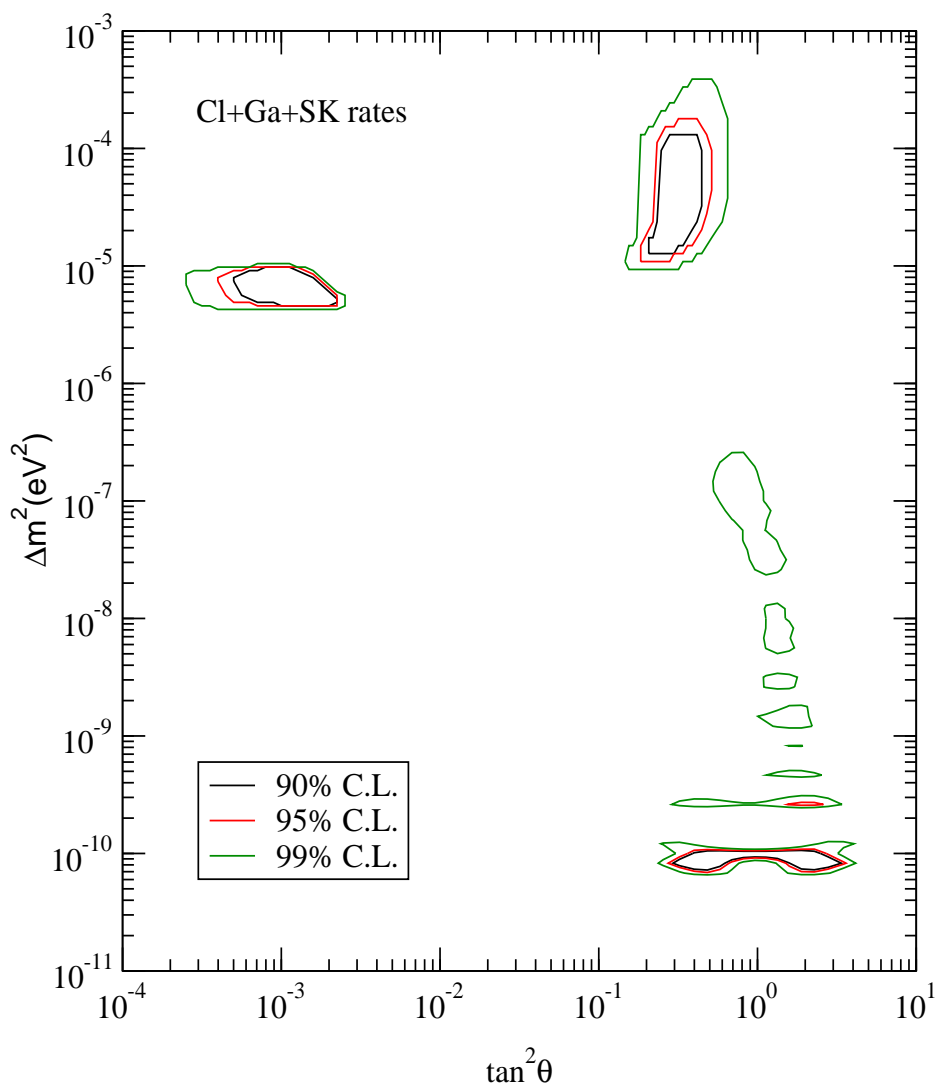


Figure 1: The pre-SNO 90%, 95% and 99% C.L. allowed area from the fit to the data on total rates from the Cl, Ga and SK experiments assuming two-generation oscillations to active neutrino.

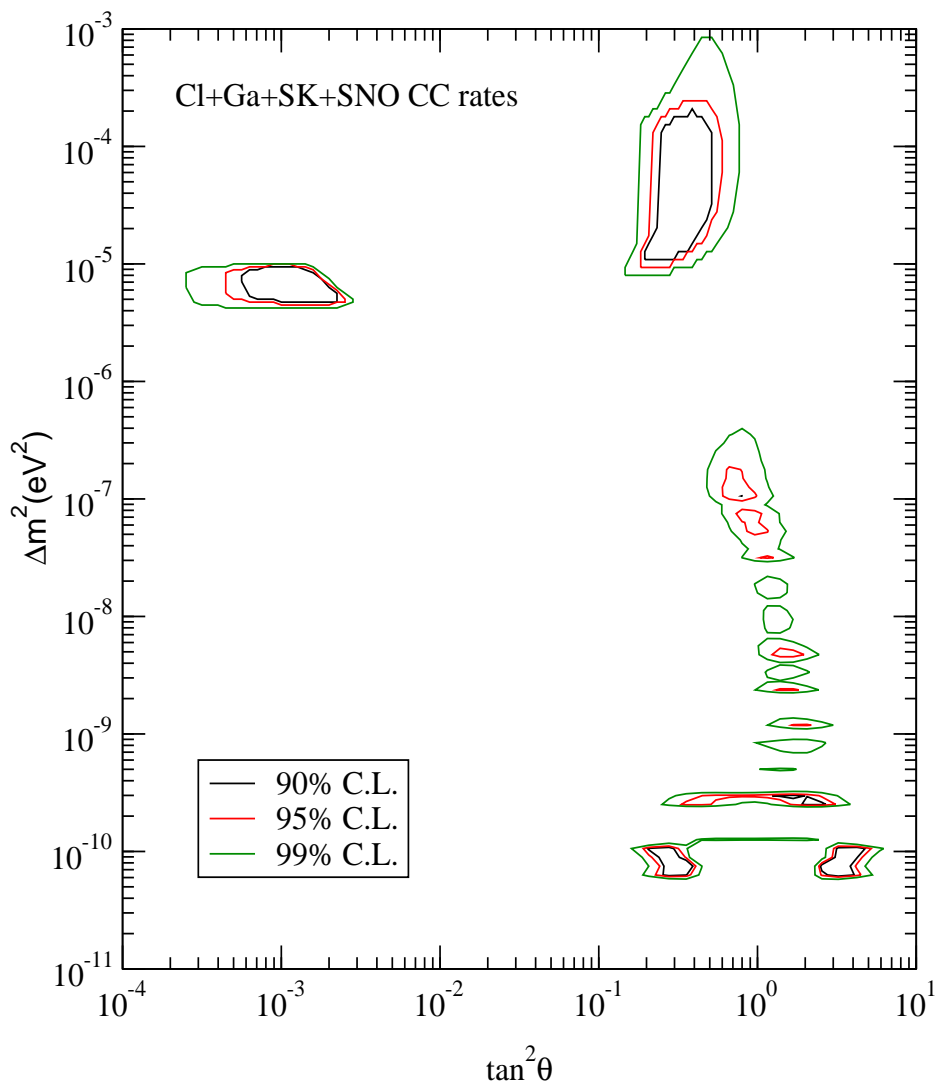


Figure 2: The post-SNO 90%, 95% and 99% C.L. allowed area from the fit to the data including the SNO CC rate along with the total rates from the Cl, Ga, SK experiments for two-generation oscillations to active neutrino.

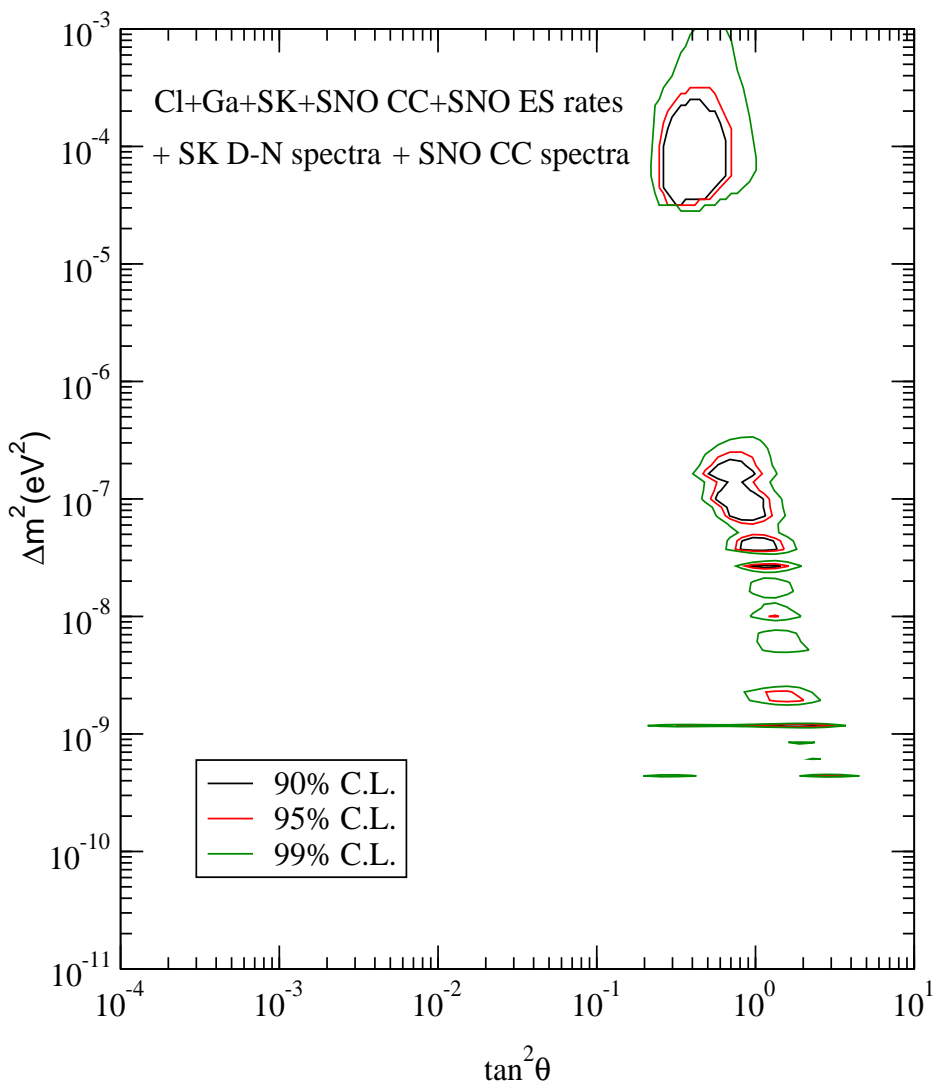


Figure 3: The post-SNO 90%, 95% and 99% C.L. allowed area from the global analysis of the total rates from Cl, Ga, SK and SNO (both CC and ES), the 1258 day SK recoil electron energy spectrum at day and night and the SNO CC spectrum data, assuming two-generation oscillations to active neutrino.